

## Fine structure in $^{14}\text{C}$ emission from $^{223}\text{Ra}$ and $^{224}\text{Ra}$

E. Hourani, L. Rosier, G. Berrier-Ronsin, A. Elayi, A. C. Mueller, G. Rappenecker,  
G. Rotbard, G. Renou, A. Lièbe, and L. Stab  
*Institut de Physique Nucléaire, F-91406 Orsay CEDEX, France*

H. L. Ravn

*Experimental Physics Division, CERN, CH-1211 Geneva 23, Switzerland*

(Received 28 March 1991)

The measurement of the energy spectrum of  $^{14}\text{C}$  nuclei emitted in the spontaneous radioactivity of  $^{223}\text{Ra}$  and  $^{224}\text{Ra}$  has been carried out, using thin and intense sources (480 MBq for  $^{223}\text{Ra}$  and 3550 MBq for  $^{224}\text{Ra}$ ). The sources were obtained by implanting mass-separated beams into Al and vitreous C catchers. The measurement was performed with a superconducting solenoidal spectrometer. Our discovery, previously reported, of fine structure in the energy spectrum of  $^{14}\text{C}$  emission from  $^{223}\text{Ra}$ , which is analogous to the one known for  $\alpha$  emission, is confirmed. Only 13% of the branching ratio in  $^{14}\text{C}$  decay leads to the ground state of the residual nucleus, while 81% to the first excited state. For  $^{14}\text{C}$  emission from  $^{224}\text{Ra}$ , a lower limit of 2 for the hindrance factor has been measured for the transition to the first excited state in the residual nucleus. Also, a precise identification in  $Z$  with an  $E \times \Delta E$  telescope has been performed for the radiation from the  $^{223}\text{Ra}$  source. Our measurements of fine structure in  $^{14}\text{C}$  emissions open this field to nuclear structure studies.

### I. INTRODUCTION

Recently (1984), natural  $^{14}\text{C}$  radioactivity was observed [1] from Ra isotopes, in parallel with  $\alpha$  decay, with branching ratios of  $\approx 10^{-10}$ . Emissions of Ne, Mg, and Si have been consecutively observed from uranium and heavier elements with branching ratios ranging from  $10^{-12}$  to  $10^{-17}$ . A common feature of all these emissions is that heavier nuclei emit heavier fragments in such a way that the daughter is always the double magic  $^{208}\text{Pb}$  or a closely neighboring nucleus. This fact is easily explained by the favorable energetic balance in the decay of heavy nuclei toward the  $^{208}\text{Pb}$  region. Two review papers of this field are given in Refs. [2] and [3].

Various techniques have been used so far. In particular, track detectors have been found to be the most appropriate to measure emissions with the lowest branching ratios. At Orsay, we used the magnetic spectrometer SOLENO to confirm [4] the first discovery, i.e., the  $^{14}\text{C}$  radioactivity of  $^{223}\text{Ra}$ , then to give evidence [5] for the  $^{14}\text{C}$  radioactivity of  $^{226}\text{Ra}$ . The logic of searching for new emitters with even smaller branching ratios ( $^{14}\text{C}/\alpha$ ) was the only rule until 1989 when, at Orsay, in an experiment with the magnetic spectrometer SOLENO, we found evidence for a fine structure in the energy spectrum of  $^{14}\text{C}$  ions emitted from  $^{223}\text{Ra}$  [6].

Concerning the theoretical aspects, fissionlike models simply relying on the  $Q$  value of the decay and on a phenomenological potential barrier have been used since 1980 and improved thereafter [7–9]. They have shown a high predictive power in the types and the branching ratios of these exotic emissions. As to whether excited states in the residual nucleus are populated or not in these emissions, the fissionlike calculations could only

evaluate the dynamical aspect, predicting an attenuation of 2 orders of magnitude for an increase of 1 MeV in excitation energy.

According to the fissionlike calculations, the decay of  $^{223}\text{Ra}$  into  $^{14}\text{C}$  goes mainly to the ground state of  $^{209}\text{Pb}$  and only with a fraction of 2% to its first excited state. The results of the fine-structure experiment of Orsay were in complete disagreement, showing a predominant transition to the first excited state (81%) and a weaker transition (15%) to the ground state. They are rather similar to the well-known results for fine structure in  $\alpha$  decay, in which transitions to the ground state in residual nuclei are hindered for odd- $A$  parent nuclei. Clearly, these facts are a strong signature of nuclear structure effects requiring microscopic calculations for their interpretation.

At present, a precise measurement of the energy spectrum of  $^{14}\text{C}$  ions emitted by Ra sources, as well as the precise identification of  $A$  or  $Z$  for such ions, are only possible by means of a spectrometer like SOLENO [10] because of both its high rejection of  $\alpha$  radiation and its large-entrance solid angle ( $\approx 200$  msr).

The significant experimental development at Orsay, after our fine-structure experiment [6], was the use of a new type of radioactive Ra source. These sources are produced by implantation at ISOLDE (CERN). Compared to our earlier sources which consisted of various chemical deposits, the new sources have higher intensities, smaller thicknesses, and better purity. These new sources produced at ISOLDE were used in the experiment which will be described in this paper, in order to confirm our preceding result obtained with  $^{223}\text{Ra}$  source and to extend it to a  $^{224}\text{Ra}$  source. In addition, a precise measurement with  $Z$  identification of the emitted radiation has been carried out using the  $^{223}\text{Ra}$  source.

## II. CHOICE OF $^{223}\text{Ra}$ AND $^{224}\text{Ra}$ SOURCES

Taking advantage of the possible production at ISOLDE of more than one source at one time, we decided to simultaneously produce two sources of  $^{223}\text{Ra}$  and  $^{224}\text{Ra}$ . Indeed, the remeasurement of  $^{223}\text{Ra}$  with a source of an alternate production type was interesting in order to confirm and to improve our earlier result. The choice of  $^{224}\text{Ra}$ , on the other hand, was based on the discussion of the Geiger-Nuttall diagram plotted for  $^{14}\text{C}$  emission from Ra isotopes, in analogy to  $\alpha$  emission.

A Geiger-Nuttall diagram consists of plotting  $\log_{10} T_{1/2}$  vs  $Q^{-1/2}$  for each emission,  $T_{1/2}$  and  $Q$  being the half-life and the  $Q$  value, respectively. Figure 1 shows the diagrams for both  $\alpha$  and  $^{14}\text{C}$  emissions from Ra isotopes. The left-hand side of the figure contains  $\alpha$  emission data taken from Ref. [17]. It is seen that transitions to the ground state and first excited state of even-even nuclei, i.e.,  $^{222}\text{Ra}$ ,  $^{224}\text{Ra}$ , and  $^{226}\text{Ra}$ , define a straight line, while data corresponding to odd- $A$  nuclei, i.e.,  $^{223}\text{Ra}$ , fall above it. The vertical deviation from the straight line is called the hindrance factor and is related to nuclear structure properties.

The right-hand side of Fig. 1 corresponds to the results of the known even-even  $^{14}\text{C}$  emitters, i.e.,  $^{222}\text{Ra}$ ,  $^{224}\text{Ra}$ , and  $^{226}\text{Ra}$  [5,11]. The  $Q$  values were calculated under the assumption that the residual nucleus has been left in its ground state. The fact that the data lie approximately on a straight line means that this assumption is almost satisfied and that the analogy with  $\alpha$  emission is meaningful. The results of the only odd- $A$   $^{14}\text{C}$  emitter, i.e.,  $^{223}\text{Ra}$ , fall above the line, similarly to  $\alpha$  emission. Now, conversely, we rely on the analogy with  $\alpha$  emission to assume that representative points of the transitions to the first excited state, for even-even  $^{14}\text{C}$  emitters, fall on the straight line in the diagram. This allows us to deduce their branching ratios, which hence have been predicted as 0.01, 2.5, and 1% of the ground state for  $^{222}\text{Ra}$ ,  $^{224}\text{Ra}$ ,

and  $^{226}\text{Ra}$ , respectively.

Our interest has been fixed on  $^{224}\text{Ra}$  among the other even-even Ra isotopes for the following reasons.

(i) For  $^{222}\text{Ra}$ , three measurements have been carried out [5,11,12]. All of them had sufficient energy resolution to resolve the first excited state of  $^{208}\text{Pb}$  at 2.6-MeV excitation energy location. No meaningful counts have been observed at this location. An appropriate search with the spectrometer SOLENO for fine structure (predicted above for this isotope to be  $\leq 10^{-5}$ ) would require unrealistic statistics.

(ii) For  $^{226}\text{Ra}$ , two measurements have been performed with the same thick source (2 mg/cm<sup>2</sup>) made at Orsay [5,20]. The thickness of the source is inherent to both the relatively high activity (2.6 mCi) of the source and its long half-life (1600 yr). The poor energy resolution expected from such a thick source together with the low branching ratio to excited states in the residual nucleus make the feasibility of the search for fine structure in  $^{226}\text{Ra}$  decay quite questionable.

(iii) For  $^{224}\text{Ra}$ , the above-predicted branching ratio (2.5%) to the first excited state is the highest, compared to those of  $^{222}\text{Ra}$  and  $^{226}\text{Ra}$ . In addition, the only previous measurement [11] for this emitter was performed in track detectors with poor statistics (22 events) and an energy resolution of about 2 MeV which is insufficient to resolve the first excited state of  $^{210}\text{Pb}$  located at 0.795-MeV excitation energy. Thus, a search for fine structure with this isotope is promising.

## III. PRODUCTION OF $^{223}\text{Ra}$ AND $^{224}\text{Ra}$ SOURCES

Radium and francium isotopes were produced by means of the ISOLDE-2 mass separator [13] at the synchrocyclotron of CERN. A 2.8- $\mu\text{A}$  proton beam of 600 MeV and a thick thorium carbide target [14] of 55 g/cm<sup>2</sup> were used during a 3-day irradiation. The  $^{223}\text{Ra}$  and  $^{224}\text{Ra}$  sources were produced by implantation of the  $A=223$  ( $^{223}\text{Ra} + ^{223}\text{Fr}$ ) and  $A=224$  ( $^{224}\text{Ra} + ^{224}\text{Fr}$ ) singly charged ions of 60 keV. The  $^{223}\text{Fr}$  and  $^{224}\text{Fr}$  isotopes are short-lived  $\beta$  emitters which transform into  $^{223}\text{Ra}$  and  $^{224}\text{Ra}$ , respectively, contributing to the production of the Ra sources. The intensities of the collected beams are displayed in Fig. 2 which shows a mass spec-

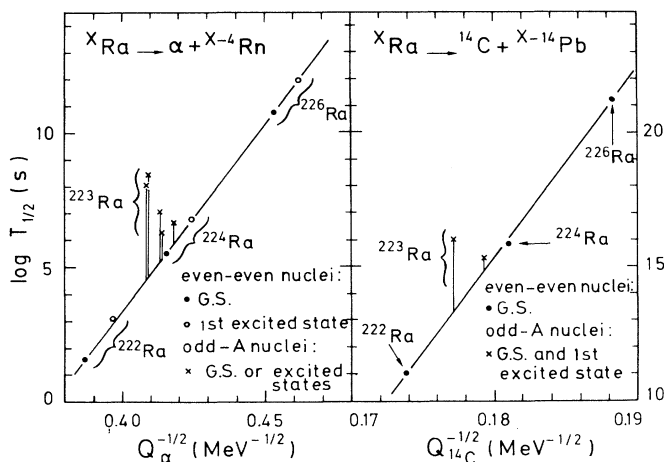


FIG. 1. Geiger-Nuttall diagram for  $\alpha$  and  $^{14}\text{C}$  emissions of Ra isotopes. The decimal logarithm of the half-lives expressed in seconds is plotted vs  $Q^{-1/2}$ , the energy balance  $Q$  of the reaction being expressed in MeV.

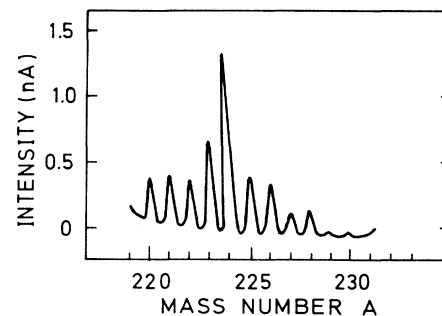


FIG. 2. The intensity of mass production at the focal chamber of ISOLDE as scanned by a wire and displayed on an oscilloscope. The peaks correspond to integer mass number  $A$  and they are composed of Fr and Ra isobars.

trum of (Ra + Fr) isotopes scanned by means of a wire at the focal chamber. The  $A=223$  ions were implanted into an Al catcher mounted in an external beam line. A uniform electrostatic scan over an area of  $15 \times 6$  mm was made. The implantation of  $A=224$  ions was performed into a vitreous carbon plate (4 mm wide and 8 mm high) placed in the focal chamber of ISOLDE. Vitreous carbon was chosen as the implantation material because of both its low coefficient of sputtering and its mechanical hardness useful for subsequent handling. Because  $^{224}\text{Ra}$  is the nearest neighbor to  $^{223}\text{Ra}$ , it was not possible to produce it simultaneously in a second beam line where a scan would have helped to decrease the consequences of the sputtering.

Indeed, sputtering of atoms from the implantation matrix is the main problem that one encounters when producing an intense source of a small area. This problem was particularly serious for the  $^{224}\text{Ra}$  source which was produced at a rate of  $8 \times 10^9$   $A=224$  ions per s. We estimated a sputtering of a total of  $10^{16}$  atoms from the carbon matrix. Assuming that the ions are implanted within a depth of 200–400 Å, an implantation area larger than  $7 \text{ mm}^2$  was required to avoid reaching the saturation in the implantation [15]. Therefore, to increase the implantation area, the beam spot was regularly moved over the carbon plate during the irradiation, horizontally by moving the carriage on which the plate was fixed, and vertically by moving the beam itself.

#### IV. CONTROL MEASUREMENT OF THE SOURCES

The aim of the control measurement was to determine the intensity of the sources and to check their isotopic purity and the energy resolution of the emitted  $\alpha$  rays. The measurement was performed, after transporting the sources rapidly to Orsay, by arranging a source and a Si detector in direct view of each other inside a vacuum chamber. The source to detector distance was made large ( $\approx 2$  m) and a diaphragm of a small diameter ( $\phi=5.5$  mm) was placed in front of the detector, so that an  $\alpha$ -counting rate of only a few hundred per s was obtained.

We first point out that, to use these sources with the spectrometer SOLENO, a 2000-Å layer of Al had to be deposited on them by evaporation. So, in the present section, after general information on  $^{223}\text{Ra}$  and  $^{224}\text{Ra}$  decay chains, we describe the  $\alpha$  spectra of the sources measured before and after the evaporation of Al.

Figures 3(a) and 4(a) give the decay chains of  $^{223}\text{Ra}$  and  $^{224}\text{Ra}$  and the most intense  $\alpha$  rays of their chain members. The rays were numbered up to 12 for  $^{223}\text{Ra}$  and up to 7 for  $^{224}\text{Ra}$ . The plot displays the intensity of these rays versus their energy (normalized to the total Ra parent intensity). One has to note the presence of a Rn isotope in each of the two decay chains. Indeed, the Rn, as a gas, will emanate from the source and will then cause various troubles.

Not only is Rn an  $\alpha$  emitter, but also it generates daughters which are themselves  $\alpha$  emitters and which, in addition, involve one member of a relatively long half-life ( $T_{1/2}=36.1$  min for  $^{211}\text{Pb}$  and 10.64 h for  $^{212}\text{Pb}$ ). Conse-

quently, when a source is handled in air, special health protection against radon is required, and when a source is measured inside a vacuum chamber, a serious  $\alpha$  radiation background from the daughters deposited on the wall of the chamber is encountered.

Figures 3(b) and 4(b) show the  $\alpha$  radiation energy spectra of  $^{223}\text{Ra}$  and  $^{224}\text{Ra}$  sources, respectively, these spectra having been established before the evaporation of Al on the sources. In Fig. 3(b), peaks labeled 11 and 12, which correspond to  $^{219}\text{Rn}$  and its next daughter  $^{215}\text{Po}$ , present two anomalies: (i) their intensities compared to those of peaks 1–6 corresponding to  $^{223}\text{Ra}$  are much higher than expected from Fig. 3(a), and (ii) they have large low-energy tails with bumps. These anomalies are due to the Rn escaping from the source and to its nearest daughter which both decay in the neighborhood of the detector into its large solid angle. Apart from these apparent anomalies, all of the expected  $\alpha$  rays are normal. In particular, the  $\alpha$  rays corresponding to  $^{223}\text{Ra}$  are well resolved and show an energy resolution of 23 keV. If we take into account the resolution of 20 keV achieved by the same detector with the 5.480-MeV  $\alpha$  ray of an  $^{241}\text{Am}$  standard source, we can say that the energy degradation due to the  $^{223}\text{Ra}$  source is small. This means that the type of source obtained by implantation at ISOLDE is of high quality and appropriate to  $\alpha$  and  $^{14}\text{C}$  emission spectroscopic studies. As to the activity of the source, it was deduced from the area of the  $^{223}\text{Ra}$  peaks and was found equal to 480 MBq (13 mCi) in  $^{223}\text{Ra}$  at the end of the irradiation.

In Fig. 4(b), corresponding to the  $^{224}\text{Ra}$  source, the peak with a low-energy tail lying between peaks 5 and 6 is spurious. It is due to  $^{211}\text{Bi}$  traces left in the vacuum chamber after the preceding measurement with the  $^{223}\text{Ra}$  source [it corresponds to peak 10 in Fig. 3(b)]. The figure displays a good quality spectrum characterized by an  $\alpha$ -ray energy resolution of 28 keV and an activity of the source of 3550 MBq (96 mCi) in  $^{224}\text{Ra}$  normalized to the end of the irradiation.

Finally, looking for common rays in the spectra of the two sources due to isotopic mixing in the production, peak 12 of the decay chain of  $^{223}\text{Ra}$  was revealed in the spectrum of  $^{224}\text{Ra}$  source and peak 7 of the decay chain of  $^{224}\text{Ra}$  was revealed in the spectrum of  $^{223}\text{Ra}$ . The cross contaminations, i.e., the activity ratio of  $^{223}\text{Ra}$  to  $^{224}\text{Ra}$  in the  $^{224}\text{Ra}$  source and of  $^{224}\text{Ra}$  to  $^{223}\text{Ra}$  in the  $^{223}\text{Ra}$  source, were determined to be  $\leq \frac{1}{1000}$  and  $\leq \frac{5}{1000}$ , respectively, at the end of the irradiation.

Figures 3(c) and 4(c) display the  $\alpha$ -ray energy spectra of  $^{223}\text{Ra}$  and  $^{224}\text{Ra}$  sources, respectively, these spectra having been measured after the evaporation of Al on the sources. In both figures, the relative height of the various peaks is in agreement with the expectation from Figs. 3(a) and 4(a). This means that most of the Rn and its daughters decay inside the source itself and, consequently, that the emanation of Rn is much lower than without the coating of Al. This analysis is reinforced by the fact that a small peak appears on the right-hand side of the radon peak [peak 11 in Fig. 3(c) and peak 5 in Fig. 4(c)]. The small peak is due to Rn nuclei decaying after emanation from the source, since its shift in energy of 40 keV

with respect to the main peak of Rn corresponds to the  $\alpha$  energy loss in the Al deposit on the source. The spurious peak on the left-hand side of peak 6 in Fig. 4(c) is due to  $^{211}\text{Bi}$  traces from the  $^{223}\text{Ra}$  source measured this time also before the  $^{224}\text{Ra}$  source. As to the energy resolution measured for the  $\alpha$  rays of Ra, the two sources gave a value of 40 keV, still quite acceptable for the success of the experiment. Unfortunately, there is a low-energy tail for  $\alpha$  rays from Ra which is more pronounced in the case of the  $^{223}\text{Ra}$  source. This may indicate that the Al evapora-

tion on the Al matrix was not as successful as on the carbon matrix.

## V. SETUP WITH SOLENO

Let us recall here that SOLENO is a superconducting coil surrounding a vacuum chamber ( $\phi=360$  mm) on the axis of which the source is placed at one side and the detector at the other side. When the electric current is set to focus on the detector  $^{14}\text{C}^{6+}$  or  $^{14}\text{C}^{5+}$  ions emitted

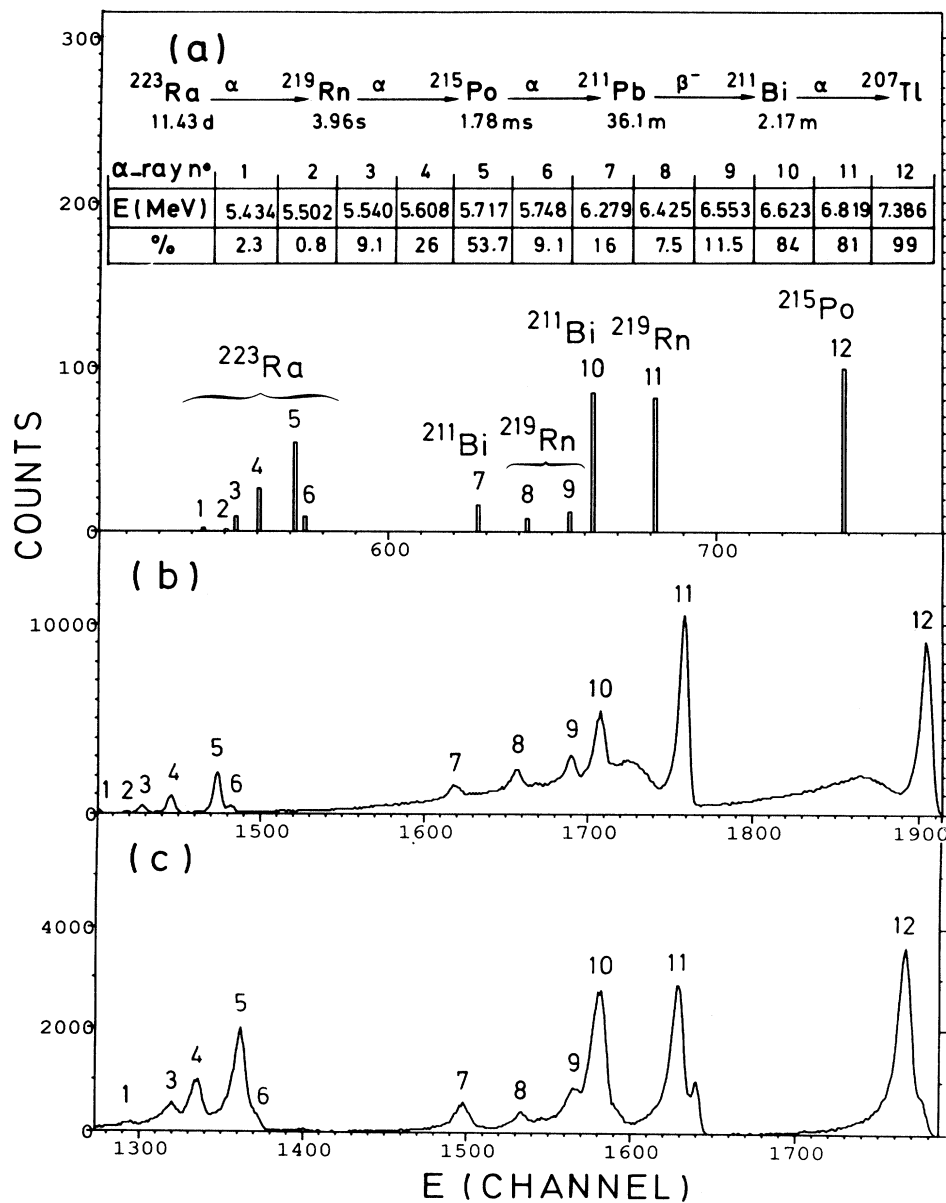


FIG. 3. The  $\alpha$ -particle spectra of the  $^{223}\text{Ra}$  source produced at ISOLDE. In (a), the decay chain of  $^{223}\text{Ra}$ , with the plot of the  $\alpha$ -ray intensities versus the  $\alpha$  energy, taken from Ref. [17]. In (b), the  $\alpha$ -ray spectrum of the  $^{223}\text{Ra}$  source produced at ISOLDE, as given by a Si surface barrier detector placed in direct view of the source. In (c), as in (b), but after the deposit of an Al layer on the source by evaporation.

by the source, the high flux of  $\alpha$  radiation emitted by the same source is focused outside the detector. A diagram of the setup is shown in Fig. 5.

**A. Transmission curve**

The focusing of SOLENO is characterized by the effective solid angle  $\Omega$  at its entrance. For a fixed source-detector geometry,  $\Omega$  depends on a single parameter  $y$  such that

$$y = B\rho/I, \tag{1}$$

where  $B\rho$  is the magnetic rigidity of the ions emitted by

the source and  $I$  is the electric current in SOLENO. The curve obtained by plotting  $\Omega$  vs  $y$  is called the transmission curve of SOLENO. For each source-detector geometry used in this work, a transmission curve has been measured, using an  $\alpha$  source of calibrated intensity and known  $B\rho$ , and varying the current  $I$  of SOLENO. The transmission curve corresponding to a quasipoint source and to a single Si detector with a  $\phi=22$  mm diaphragm in front is shown in Fig. 6. The same figure indicates the current values used in the various measurements and the locations (indicated with arrows) corresponding to the  $^{14}\text{C}$  ions which populate the low-lying excited states in the residual nucleus.

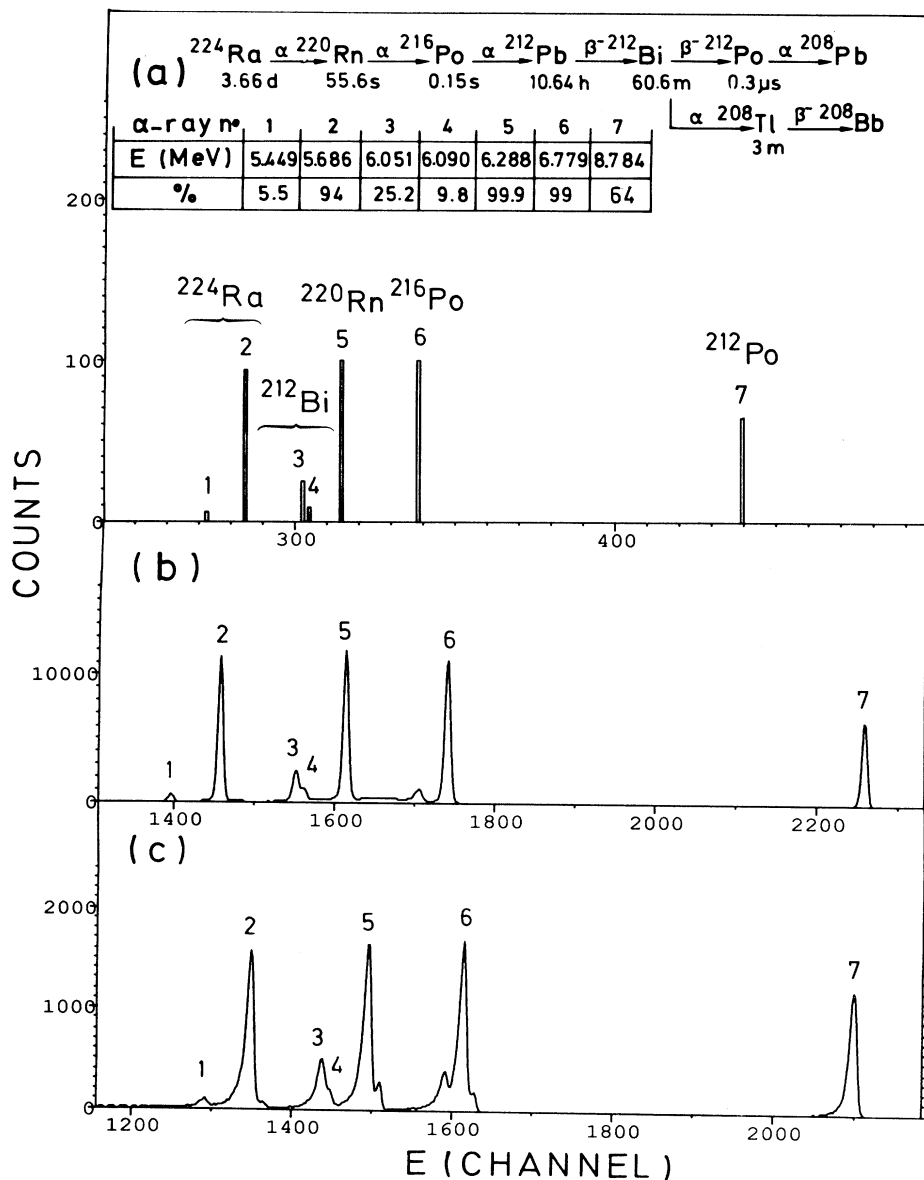


FIG. 4. As in Fig. 3, but for the  $^{224}\text{Ra}$  source produced at ISOLDE.

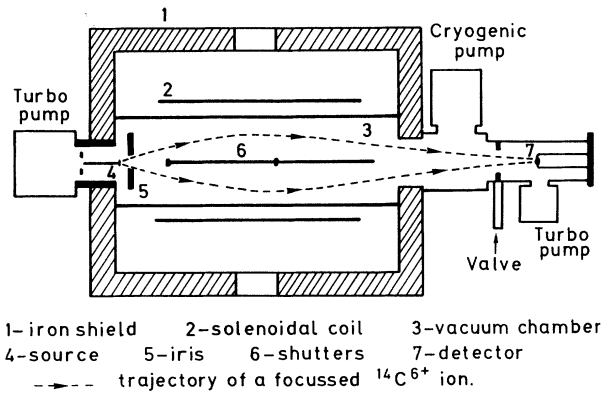


FIG. 5. The setup with SOLENO. The drawing shows the mechanical structure of SOLENO: the coil, the iron shield, and the vacuum chamber. The vacuum pumping and the source detector configuration with ion trajectories are shown.

### B. Detectors

In the search for fine structure in the energy spectrum of  $^{14}\text{C}$  ions from  $^{223}\text{Ra}$  and  $^{224}\text{Ra}$ , a single Si detector was used in order to reach the best energy resolution. It was a passivated implanted planar detector (made by Canberra), partially depleted, with a thickness of  $100\ \mu\text{m}$  and an area of  $450\ \text{mm}^2$ . Its energy resolution was  $18\ \text{keV}$  for  $\alpha$  particles and  $110\ \text{keV}$  for  $^{12}\text{C}$  particles of  $30\ \text{MeV}$ .

A surface barrier Si detector telescope, manufactured at the Institut de Physique Nucléaire (IPN) of Orsay, was used for  $Z$  identification. The  $E$  detector was partially depleted,  $300\ \mu\text{m}$  thick, with an area of  $450\ \text{mm}^2$ . The

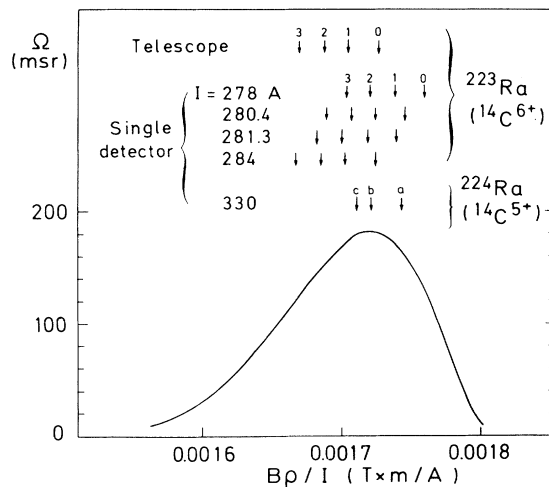


FIG. 6. The transmission curve of SOLENO, with a  $\phi=22$  mm diaphragm in front of the detector. The solid angle  $\Omega$  of SOLENO is given as function of the parameter  $y = B\rho/I$ , where  $B\rho$  is the magnetic rigidity of the ions emitted by the source and  $I$  is the current in SOLENO. The locations of the ground state and some low-lying excited states in the residual nucleus of the decay of  $^{223}\text{Ra}$  and  $^{224}\text{Ra}$  are labeled with numbers and letters, respectively.

$\Delta E$  detector was of epitaxial type, totally depleted,  $9\ \mu\text{m}$  thick, with an area of  $250\ \text{mm}^2$ . A detailed description of the  $\Delta E$  detector is given in Fig. 6 of Ref. [16].

### C. $\alpha$ background

A serious problem expected to occur in the measurement of such intense sources with SOLENO is an intense background from  $\alpha$  particles. This may cause strong multiple pileup and even rapidly damage the detector.

One origin of  $\alpha$  particles is radon emitted from the source and traveling as a neutral gas inside the vacuum chamber of SOLENO. The radon and its daughters decay in the neighborhood of the detector producing an overall  $\alpha$  background which is independent of the current setting of SOLENO but proportional to the detector area. In order to reduce this type of background, an efficient pumping with two turbomolecular pumps in addition to the standard cryogenic pump was used. Also, a diaphragm ( $\phi=16\ \text{mm}$ ) designed to cover half of the detector area was prepared.

The other origin of  $\alpha$  particles falling on the detector is the source itself which emits a tremendous flux of energetic ( $5-8\ \text{MeV}$ ) singly or doubly charged  $\alpha$  radiation. In the previous uses of SOLENO, the current was set for a magnetic rigidity  $B\rho$  of  $^{14}\text{C}^{6+}$  at the maximum of the transmission curve. This was not possible for the source of  $^{224}\text{Ra}$  because of the proximity of the  $B\rho$  of  $8.784\ \text{MeV}$   $\alpha^{++}$  emitted by  $^{216}\text{Po}$ , which is a member of the decay chain of  $^{224}\text{Ra}$ . Therefore, the  $^{14}\text{C}^{5+}$  state was used in our measurement.

### D. Charge-state distribution

We needed to know the percentages of  $^{14}\text{C}^{5+}$  and  $^{14}\text{C}^{6+}$  charge states in an interval of a few MeV around a  $^{14}\text{C}$  ion energy of  $30\ \text{MeV}$ . Under the assumption that  $^{12}\text{C}$  and  $^{14}\text{C}$  atoms of equal velocity have approximately the same charge-state distributions, we measured such distributions for a  $^{12}\text{C}$  beam of about  $25\ \text{MeV}$  delivered by the Tandem at Orsay. To simulate the Al deposit on  $^{223}\text{Ra}$  and  $^{224}\text{Ra}$  sources, the  $^{12}\text{C}$  beam had to traverse an Al foil of  $100\ \mu\text{g}/\text{cm}^2$ .

Two methods of measurement were performed. In one simple method, the analyzed  $^{12}\text{C}^{4+}$  beam of the Tandem was allowed to cross an Al foil of  $100\ \mu\text{g}/\text{cm}^2$ . At the exit of the foil, the charge equilibrated  $^{12}\text{C}^{6+}$ ,  $^{12}\text{C}^{5+}$ , and  $^{12}\text{C}^{4+}$  beams were consecutively switched towards a Faraday cup and their intensity measured. In the second method, the  $^{12}\text{C}^{4+}$  beam hit a  $100\text{-}\mu\text{g}/\text{cm}^2$  Al target and the elastically scattered  $^{12}\text{C}^{6+}$  and  $^{12}\text{C}^{5+}$  ions were focused with a split-pole spectrometer placed at  $9^\circ$  and measured with a multiwire proportional counter. The two methods were in agreement.

The results of the two measurements are plotted in Fig. 7 together with the results for a  $^{12}\text{C}$  beam incident on a C foil taken from the compilation of Shima *et al.* [18] and connected by continuous lines. We read the percentages of  $5^+$  and  $6^+$  charge states on the dashed curves which are parallel to the continuous lines and also fit our two results. The data measured by Kutschera *et al.* [19] at Argonne are also shown on the same figure. They are in agreement with our results.

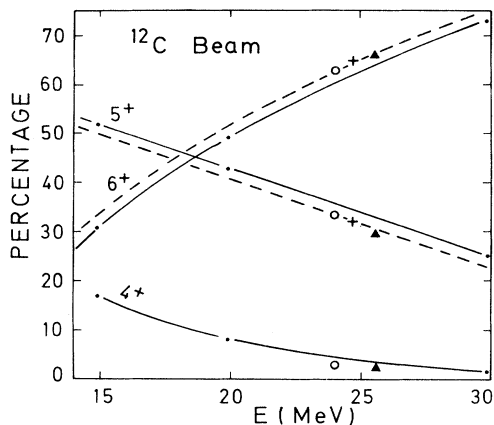


FIG. 7. The charge-state distribution plotted against the kinetic energy for  $^{12}\text{C}$ . The continuous line connects three points taken from Ref. [18] and given for a  $^{12}\text{C}$  beam incident on a C foil. The symbols  $\circ$  and  $+$  represent two measurements we have performed for a  $^{12}\text{C}$  beam incident on a  $100\text{-}\mu\text{g}/\text{cm}^2$  Al foil. The symbol  $\blacktriangle$  represents the results of Kutschera *et al.* [19] for a  $^{14}\text{C}$  beam incident on a  $100\text{-}\mu\text{g}/\text{cm}^2$  Al foil.

#### VI. FINE STRUCTURE IN $^{14}\text{C}$ RADIOACTIVITY OF $^{224}\text{Ra}$

In a preliminary measurement, the current of SOLENO was set to focus  $^{14}\text{C}^{5+}$  ions. The counting rate of  $\alpha$  particles originating from radon was too high and, in addition, noticeable traces of  $^{224}\text{Ra}$  sputtered from the source were detected. Having realized that both troubles originated from the location of Ra atoms on the surface of the source (due to the removal of the  $200\text{-}\text{\AA}$  matrix layer by sputtering during the irradiation), we decided to deposit on the source a  $2000\text{-}\text{\AA}$  layer of Al, in order to reduce the emanation of radon and to prevent the sputtering of Ra. The deposit was achieved successfully. The emanation of radon was reduced by a factor of 5. The sputtering of Ra was completely stopped and the energy resolution in the  $\alpha$  spectrum measured in direct view of the source was only slightly degraded from 28 to 40 keV.

The measurement with SOLENO consisted of a 6.3-d run, the current of SOLENO being set at the value of 330 A which focuses  $^{14}\text{C}^{5+}$  ions emitted from  $^{224}\text{Ra}$ . Having started the measurement with a diaphragm of  $\phi=16$  mm placed in front of the detector, this diaphragm was exchanged for another one of  $\phi=22$  mm, 2.2 d later when the activity of the source had decreased by a factor of 1.5.

Throughout the measurement, the multiple pileup was closely controlled. Indeed, taking into account the energy range (5.449–8.784 MeV) of the  $\alpha$  rays generated by  $^{224}\text{Ra}$  and the members of its decay chain, the triple pileup was expected to extend in energy to an upper edge of 26.353 MeV, which is due to the triple pileup of the 8.784-MeV  $\alpha$  ray. On the other hand, as the energy of  $^{14}\text{C}$  ions feeding the ground state of the residual nucleus  $^{210}\text{Pb}$  is 28.631 MeV, an interval of 2.3 MeV was left between the ground-state position and the upper limit of

the triple pileup to observe the four low-lying excited states in  $^{210}\text{Pb}$ . In fact, the measured  $\alpha$  counting rate did not exceed 3000 counts/s during the experiment. The quadruple pileup which could disturb our measurement was 9 orders of magnitude lower. So, only a few counts, i.e., not more than 3 or 4, could have occurred during the whole measurement and, in addition, these should have fallen over a wide range of energy.

Transmission curves of SOLENO were established before and after the measurement for the two diaphragms of  $\phi=16$  and 22 mm used consecutively in front of the detector. The curve corresponding to the  $\phi=22$  mm diaphragm was found to be 1.41 times the other. This curve is presented in Fig. 6, where the arrows indicate the locations of the ground state (label *a*) and the first and the second excited states (labels *b* and *c*) of  $^{210}\text{Pb}$ . The current setting of SOLENO was chosen to place the excited states at the maximum of the transmission curve.

The results of the measurement are reported in Fig. 8, where a very sharp peak is seen. The peak contains 149 events. It shows an energy resolution of 150 keV. It is located exactly at the position expected for the ground state of  $^{210}\text{Pb}$ , as deduced from the energy calibration with  $^{14}\text{C}$  emission from a  $^{223}\text{Ra}$  source. We conclude that this peak corresponds to the transition from  $^{224}\text{Ra}$  by  $^{14}\text{C}$  radioactivity towards the ground state of the residual nucleus  $^{210}\text{Pb}$ . At the left of the figure a few triple pileup events are seen and the upper edge of the triple pileup is indicated. In between the  $^{14}\text{C}$  ground-state peak and the  $\alpha$  triple pileup region, the locations of the four low-lying excited states of  $^{210}\text{Pb}$  are indicated with arrows. No

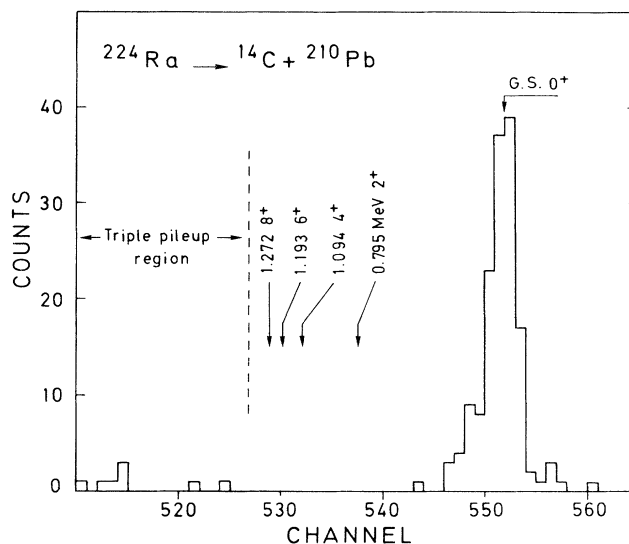


FIG. 8. The energy spectrum of  $^{14}\text{C}$  ions measured with the  $^{224}\text{Ra}$  source. The arrows indicate the locations of the ground state and some low-lying excited states in the residual nucleus  $^{210}\text{Pb}$ . No events are seen at the locations of the excited states. The energy calibration has been deduced from the peak positions for the  $^{223}\text{Ra}$  source, the latter having been calibrated in a previous experiment with a  $^{14}\text{C}$  beam from the Tandem of Orsay. The energy resolution is 150 keV.

events at all are seen at these locations. This fact means that, within the sensitivity of our experiment, no transition from  $^{224}\text{Ra}$  by  $^{14}\text{C}$  emission towards the low-lying excited states of  $^{210}\text{Pb}$  is observed.

We calculated for  $^{224}\text{Ra}$  the branching ratio  $B$  of  $^{14}\text{C}$  emission with respect to  $\alpha$  decay according to the following formula:

$$n = BN\Omega\epsilon/4\pi, \quad (2)$$

where  $n$  is the number of  $^{14}\text{C}$  nuclei detected (149),  $N$  is the total number of  $^{224}\text{Ra}$  nuclei which decayed during the measurement ( $5.01 \times 10^{14}$ ),  $\Omega$  is the effective solid angle of SOLENO (161 msr for a  $\phi=22$  mm diaphragm), and  $\epsilon$  is the  $5^+$  charge-state percentage of the  $^{14}\text{C}$  ions emitted by  $^{224}\text{Ra}$  (at 28 MeV, a value of 32.5% has been used). Taking into account the numerical values and the change in transmission for two different diaphragms, a branching ratio ( $^{14}\text{C}/\alpha$ ) of  $(6.5 \pm 1.0) \times 10^{-11}$  has been deduced. It is slightly higher than the only one previously reported [11] [ $(4.3 \pm 1.2) \times 10^{-11}$ ]. Nevertheless, both results are in agreement within their respective uncertainties. On the other hand, as no event was detected for the first excited state of  $^{210}\text{Pb}$ , a lower limit of 2 for the hindrance factor (confidence level of 90%) has been deduced. Two final conclusions can be drawn: (i) a sensitivity in  $^{14}\text{C}$  emission measurement to a branching ratio of  $4 \times 10^{-13}$  with respect to  $\alpha$  decay has been reached; this is a record for the setup with SOLENO, and (ii) the nuclear structure origin of the measured hindrance factor limit appeals for a spectroscopic interpretation.

## VII. CONFIRMATION OF THE FINE STRUCTURE IN $^{14}\text{C}$ EMISSION FROM $^{223}\text{Ra}$

Our main goal with the  $^{223}\text{Ra}$  source was a confirmation of our previous result [6] which gave evidence for fine structure. Naturally, we also tried to achieve better statistics and a better energy resolution. On the other hand, the present measurement with the  $^{223}\text{Ra}$  source immediately followed the one with the  $^{224}\text{Ra}$  source. The same detection conditions for the two sources were maintained in order to have an identical energy calibration.

Five successive runs have been carried out for different values of the current in SOLENO. The current values have been chosen such that the transitions towards the ground state (label 0) and the excited states (labels 1, 2, and 3) in  $^{209}\text{Pb}$  (Fig. 6) had various locations on the transmission curve.

A total number of 700 events was detected, twice the statistics of our previous measurement [6]. The energy spectrum is given in Fig. 9. Two prominent peaks are clearly present. They correspond to the ground state and to the first excited state in  $^{209}\text{Pb}$ . This result definitely confirms the fine structure in the energy spectrum of  $^{14}\text{C}$  radioactivity from  $^{223}\text{Ra}$ .

The main part of the peaks has a width of 150 keV, which is better than our previous value of 240 keV. Unfortunately, the shape of the peaks is not Gaussian and

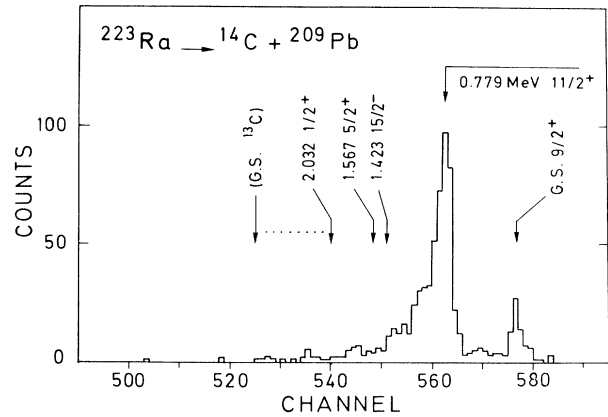


FIG. 9. The energy spectrum of  $^{14}\text{C}$  ions measured with the  $^{223}\text{Ra}$  source. The arrows indicate the locations of the ground state and some low-lying excited states in the residual nucleus  $^{209}\text{Pb}$ . The presence of the peak at 0.779 MeV is the unambiguous confirmation of the evidence for a fine structure. The main parts of the  $^{14}\text{C}$  rays show a resolution in energy of about 150 keV.

there is a low-energy tail, which is larger than in the case of  $^{224}\text{Ra}$  source, as expected from the  $\alpha$ -ray control spectra (see Sec. IV). As no peak of the characteristic width (150 keV) is seen over the location of the second and higher excited states, we can conclude that none of these has been detected.

Nevertheless, it should be interesting to repeat this experiment in the near future with improved sensitivity. This should be possible after the installation of ISOLDE at CERN's Proton Synchrotron (PS) booster. We plan to do it, benefitting from our experience gained in the choice of source implantation matrices and in the control of Al depositions.

For the calculation of the branching ratio ( $^{14}\text{C}/\alpha$ ), we label a given run with an index  $i$  specifying the current of SOLENO and call  $N_i$  the total number of  $^{223}\text{Ra}$  nuclei which have decayed. Furthermore, the excitation energies in  $^{209}\text{Pb}$  is divided into intervals labeled  $j$ . With this notation, the branching ratio  $B_j$  is given by

$$n_{ij} = B_j N_i \Omega_{ij} \epsilon_j / 4\pi, \quad (3)$$

where the quantity  $n_{ij}$  is the number of  $^{14}\text{C}$  nuclei which were measured in the interval  $j$  during the run  $i$ ,  $\Omega_{ij}$  is the effective solid angle of SOLENO corresponding to the interval  $j$  in the run  $i$ , and  $\epsilon_j$  is the  $6^+$  charge-state percentage of the  $^{14}\text{C}^{6+}$  ions populating the interval  $j$ .

The total  $^{14}\text{C}$  emission branching ratio with respect to  $\alpha$  emission was found to be  $(7.0 \pm 0.4) \times 10^{-10}$ , whereas the branching ratio to the ground state of  $^{209}\text{Pb}$  was equal to  $(0.91 \pm 0.20) \times 10^{-10}$  instead of the value  $6 \times 10^{-10}$  previously used in predictive models. The partial branching ratios to the ground state and to the first excited state of the residual nucleus have been deduced to be  $13 \pm 3\%$  and  $81 \pm 6\%$ , respectively. All these numbers concerning the various calculated branching ratios are in agreement with those obtained in our first measurement (Table I) and do not appreciably modify Fig. 1 which is based on our previous results. In Fig. 10, we report for compar-

TABLE I. Comparison of the branching-ratio results of this work and of previous works.

Parent nucleus	Daughter nucleus	$B(^{14}\text{C}/\alpha)$		Ref.
		This work	Other works	
$^{224}\text{Ra}$	$^{210}\text{Pb}$ g.s.	$(6.5 \pm 1.0) \times 10^{-11}$	$(4.3 \pm 1.2) \times 10^{-11}$	[11]
$^{224}\text{Ra}$	$^{210}\text{Pb}$ $E_x = 0.795$ MeV	$\leq 4 \times 10^{-13}$		
$^{223}\text{Ra}$	$^{209}\text{Pb}$ g.s.	$(0.9 \pm 0.2) \times 10^{-10}$	$(1.0 \pm 0.2) \times 10^{-10}$	[6]
$^{223}\text{Ra}$	$^{209}\text{Pb}$ $E_x = 0.779$ MeV	$(5.7 \pm 0.4) \times 10^{-10}$	$(5.2 \pm 0.4) \times 10^{-10}$	[6]

ison our old result together with the present ones. We note that both results exhibit a moderate sensitivity to the detection of higher excited states with smaller branching ratios, due to low-energy tailing.

### VIII. IDENTIFICATION WITH A TELESCOPE

In the previous measurements of  $^{14}\text{C}$  emission, either with track detectors or with Si telescopes, none was focused on a search for fine structure in the atomic number  $Z$  of the emitted light nuclei. The measurement described hereafter is the first to have been optimized in statistics and in detection quality to be sensitive to a few percent in fine structure in  $Z$ .

The source of  $^{223}\text{Ra}$  was used and the single detector was replaced by the Si  $E \times \Delta E$  telescope. The current of SOLENO was set to the value of 284 A already used to focus  $^{14}\text{C}^{6+}$  ions emitted by  $^{223}\text{Ra}$ . The focusing is illustrated by the positions of the arrows on the transmission curve in Fig. 6.

A 6-d measurement was performed. A total of 210 events were recorded and are given in a bidimensional  $E \times \Delta E$  plot (Fig. 11). It should be noticed that in this diagram the quantity  $E$  is the response of the back detector, i.e., the residual energy, instead of the total energy more conventionally used in the literature. A small size dot represents a single event whereas a big size dot represents a set of 10 grouped events. It is seen that more than one-

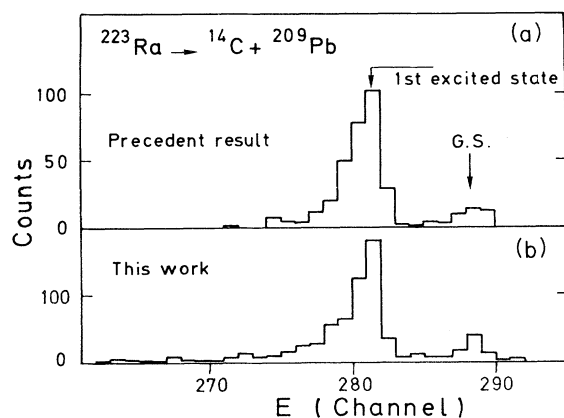


FIG. 10. Comparison of our previous result which gave evidence for the fine structure and of the present result which confirmed the discovery. The statistics in the present result are twice as high and the energy resolution is better. Low-energy tailing in both results is seen.

half of the total number of events are concentrated over a small region, while the rest are mainly spread along two lines, one line being horizontal and the other with a slope such that  $E \times \Delta E = \text{const}$ . In the same figure, there are reported the results of a calibration with  $^{12}\text{C}$  and  $^{16}\text{O}$  beams of different energies delivered by the Orsay Tandem. Contour limits at  $\frac{1}{5}$  and  $\frac{1}{50}$  of the maximum of the telescope response to each beam have been drawn.

In an overall comparison, it clearly appears the C and O beam locations fall on two distinct horizontal lines and that the  $^{223}\text{Ra}$  source results lie very close to the 29-MeV C beam position (the shift in the location was caused by electronic signal attenuation due to longer cables for the measurement with beams). This fact illustrates the conclusion that at least a large part of the  $^{223}\text{Ra}$  source results corresponds to C and not to O or other ions. Now, analyzing the spread of the source results, one can explain the horizontal extension by the natural width in energy of  $^{14}\text{C}$  nuclei emitted by  $^{223}\text{Ra}$ . As to the few events distributed over the  $E \times \Delta E = \text{const}$  line, they are compatible with C ions having undergone channeling in the  $\Delta E$  detector. Thus, at the present level of statistics, no fine structure in  $Z$  was visible.

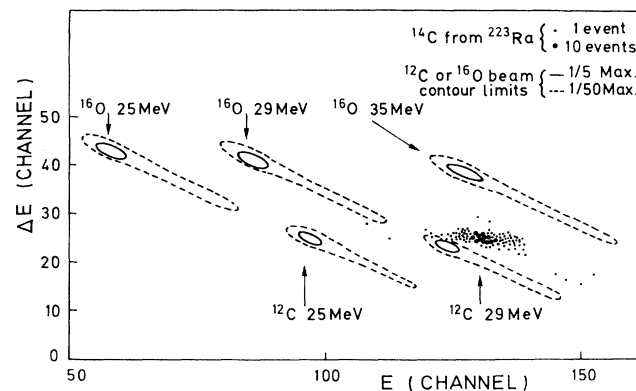


FIG. 11. The  $E \times \Delta E$  bidimensional spectrum obtained with the  $^{223}\text{Ra}$  source. The dots represent the detected events. The contour plots represent the response of the telescope to  $^{12}\text{C}$  and  $^{16}\text{O}$  beams of various energies delivered by the Orsay Tandem. As expected, the event location is very close to the 29-MeV C beam. The small shift in energy has an electronic attenuation origin due to longer cables used in the measurement with beam. The  $E \times \Delta E = \text{const}$  slope, either in the measurement with the source or in the one with the beams, is due to channeling in the  $\Delta E$  detector.

## IX. DISCUSSION AND CONCLUSIONS

The present work combined two unique facilities, ISOLDE as a source production system and SOLENO as a large solid angle (200 msr) spectrometer. The quality criteria of the sources are the energy resolution for  $\alpha$  rays and the isotopic purity. The  $\alpha$  energy resolution measured in this work was excellent and very close to the limiting value ( $\approx 20$  keV) obtained with standard  $\alpha$  sources. As to the cross contamination by neighboring Ra isotopes, it did not exceed a few parts per thousand.

On the other hand, one had to suspect that the sputtering during the implantation sets a saturation limit on the activity, in the production of sources with small areas (a few units to a few tens of  $\text{mm}^2$ ). In fact, the saturation should be reached beyond several days of irradiation, which is too long a period for a normal irradiation request at ISOLDE.

Indeed, in the first measurement of the  $\alpha$  spectrum of the  $^{224}\text{Ra}$  source, we realized that the intensity of this source was exceptional and hence appropriate to overcome the weak  $^{14}\text{C}$  emission from  $^{224}\text{Ra}$  (1 order of magnitude lower than that from  $^{223}\text{Ra}$ ). So, despite difficult handling due to the presence of a long half-life daughter ( $^{212}\text{Pb}$ ,  $T_{1/2} = 10.64$  h) and a high-energy  $\gamma$  emitter ( $^{208}\text{Tl}$ ,  $E_\gamma = 2.6$  MeV) in the decay chain of the emanating radon, a very precise result has been obtained, clearly improving the previously measured value for the branching ratio of  $^{14}\text{C}$  emission from  $^{224}\text{Ra}$  and giving evidence for the existence of a hindrance factor in  $^{14}\text{C}$  emission to the first excited state in the residual nucleus.

The measurement of the  $^{223}\text{Ra}$  source served three purposes. The first was to confirm the fine structure in the energy spectrum of  $^{14}\text{C}$  emission from  $^{223}\text{Ra}$  that we have discovered using a chemically deposited  $^{227}\text{Th}$  source. The fine-structure result was unambiguously reproduced with the new type of  $^{223}\text{Ra}$  source. The second purpose was to carry out a precise identification in Z. This also was successfully achieved and showed that all the events fall at the C location as determined with a C beam. The final purpose was the use of the ground-state location in the energy spectrum in order to calibrate the energy scale in the  $^{224}\text{Ra}$  measurement. Indeed, with this calibration, the observed peak in the  $^{224}\text{Ra}$  measurement came at the ground-state location expected for  $^{14}\text{C}$  ions emitted from  $^{224}\text{Ra}$  nuclei.

During this work, we have experimented with the production, the handling, and the measurement with SOLENO of Ra sources produced at ISOLDE. In particular, we have gained experience with two different implantation matrices, i.e., Al and vitreous carbon, and the Al evaporation on the sources. After our present success, we plan to perform a further experiment with, again, a

$^{223}\text{Ra}$  source under optimized conditions to attain an ultimate energy resolution. Such resolution together with good statistics are required to resolve the second and higher excited states in the residual nucleus. In addition, a precise measurement would tell us if there are events occurring in the energy spectrum at the location of  $^{13}\text{C}$  emitted from  $^{223}\text{Ra}$ . Such an occurrence was suggested by the mass identification results of Kutschera *et al.* [19] which yielded one event out of 24 at the  $^{13}\text{C}$  location.

Already in 1986, the plot of the branching ratio of  $^{14}\text{C}$  emissions versus the mass number of the parent nucleus showed an odd-even effect analogous to that for  $\alpha$  emission [20]. At present, we explain this odd-even effect as a manifestation of a large hindrance for transitions from odd- $A$  parent nuclei to the ground state of their daughter nuclei. In particular, we expect  $^{231}\text{Pa}$  and  $^{233}\text{U}$ , which are odd- $A$  Ne emitters, to have in their decays transitions toward the excited states of their daughters.

In fact, only the outlines of this type of radioactivity have been explained so far [8,9]. It has been explained as a superasymmetric fission toward the  $^{208}\text{Pb}$  region governed by the  $Q$  value of the decay and by an appropriate potential barrier. This fission reproduces approximately the absolute branching ratios but fails in the explanation of the observed hindrance factors which are connected to the overlapping of microscopic wave functions of the parent nucleus and the emitted fragments. A microscopic calculation similar to the one initiated by Blendowske *et al.* [21,22] should be developed. It has to explain not only the transition observed from  $^{223}\text{Ra}$  to the first excited state of  $^{209}\text{Pb}$ , but also the hindrance which we have observed in this work from  $^{224}\text{Ra}$  to the first excited state in  $^{210}\text{Pb}$ . It is probably such a hindrance with a nuclear structure origin which has also lowered the  $^{14}\text{C}$  emission from  $^{221}\text{Fr}$  and  $^{221}\text{Ra}$  in such a way that they have not been observed yet [20].

## ACKNOWLEDGMENTS

We are obliged to H. Sergolle for his constant attention to the success of this experiment. We thank A. Traverse for valuable discussions on the sputtering. We thank, also, D. Sznajderman who successfully deposited, by evaporation, the Al layer on the sources. We acknowledge the help of J. Geurtz in furnishing liquid helium and of R. Bzyl in the preparation of the Si detectors. We are grateful to the crew of the synchrocyclotron and of ISOLDE at CERN for the excellent running of these facilities that allowed the production of high-quality sources. We thank R. Deltenre at CERN for his help in handling the sources and the health service staff at the IPN of Orsay for their constant presence during the experiment. We also thank the crew of the Orsay Tandem.

- 
- [1] H. J. Rose and G. A. Jones, *Nature (London)* **307**, 245 (1984).  
 [2] E. Hourani, M. Hussonnois, and D. N. Poenaru, *Ann. Phys. (Paris)* **14**, 311 (1989).  
 [3] P. B. Price, *Annu. Rev. Nucl. Part. Sci.* **39**, 19 (1989).

- [4] S. Gales, E. Hourani, M. Hussonnois, J. P. Schapira, L. Stab, and M. Vergnes, *Phys. Rev. Lett.* **53**, 759 (1984).  
 [5] E. Hourani, M. Hussonnois, L. Stab, L. Brillard, S. Gales, and J. P. Schapira, *Phys. Lett.* **160B**, 375 (1985).  
 [6] L. Brillard, A. G. Elayi, E. Hourani, M. Hussonnois, J. F.

- Le Du, L. H. Rosier, and L. Stab, *C. R. Acad. Sci. Paris* **309 II**, 1105 (1989).
- [7] A. Sandulescu, D. N. Poenaru, and W. Greiner, *Fiz. Elem. Chastits At. Yadra* **11**, 1334 (1980) [*Sov. J. Part. Nucl.* **11**, 528 (1980)].
- [8] D. N. Poenaru, M. Ivascu, A. Sandulescu, and W. Greiner, *Phys. Rev. C* **32**, 572 (1985).
- [9] Y. J. Shi and W. J. Swiatecki, *Phys. Rev. Lett.* **54**, 300 (1985).
- [10] J. P. Schapira, F. Azaiez, S. Fortier, S. Gales, E. Hourani, J. Kumpulainen, and J. M. Maison, *Nucl. Instrum. Methods* **224**, 337 (1984).
- [11] P. B. Price, J. D. Stevenson, S. W. Barwick, and H. L. Ravn, *Phys. Rev. Lett.* **54**, 297 (1985).
- [12] M. Hussonnois, J. F. Le Du, L. Brillard, J. Dalmaso, and G. Ardisson, Report No. IPNO-DRE 9107, IPN, 91406 Orsay Cedex.
- [13] H. L. Ravn, *Phys. Rep.* **54**, 201 (1979).
- [14] T. Bjornstad, L. C. Carraz, H. A. Gustafsson, J. Heinemeier, B. Jonson, O. C. Jonsson, V. Lindfors, S. Mattsson, and H. L. Ravn, *Nucl. Instrum. Methods* **186**, 391 (1981).
- [15] The implantation was simulated using code TRIM. J. F. Ziegler, J. P. Biersack, and U. Littmark, *The Stopping and Range of Ions in Solids* (Pergamon, New York, 1985).
- [16] L. Stab, *Nucl. Instrum. Methods A* **288**, 24 (1990).
- [17] *Tables of Isotopes*, edited by C. M. Lederer and V. S. Shirley, 7th ed. (Wiley, New York, 1978).
- [18] K. Shima, T. Mikumo, and H. Tawara, *At. Data Nucl. Data Tables* **34**, 357 (1986).
- [19] W. Kutschera *et al.*, *Phys. Rev. C* **32**, 2036 (1985).
- [20] S. W. Barwick, P. B. Price, H. L. Ravn, E. Hourani, and M. Hussonnois, *Phys. Rev. C* **34**, 362 (1986).
- [21] R. Blendowske, T. Fliessbach, and H. Walliser, *Nucl. Phys. A* **464**, 75 (1987).
- [22] R. Blendowske and H. Walliser, *Phys. Rev. Lett.* **61**, 1930 (1988).